

Lightly Doped t - J Three-Leg Ladders

- an Analog for the Underdoped Cuprates

T.M. Rice⁽¹⁾, Stephan Haas⁽¹⁾, Manfred Sigrist^{(1)*}, and Fu-Chun Zhang⁽²⁾

⁽¹⁾ *Theoretische Physik, ETH-Hönggerberg, CH-8093 Zürich, Switzerland*

⁽²⁾ *Department of Physics, University of Cincinnati, Cincinnati, OH 45221*

(February 1, 2008)

Abstract

The three-leg ladder has one odd-parity and two even-parity channels. At low doping these behave quite differently. Numerical calculations for a $t - J$ model show that the initial phase upon hole doping has two components - a conducting Luttinger liquid in the odd-parity channel, coexisting with an insulating (i.e. undoped) spin liquid phase in the even-parity channels. This phase has a partially truncated Fermi surface and violates the Luttinger theorem. This coexistence of conducting fermionic and insulating paired bosonic degrees of freedom is similar to the recent proposal of Geshkenbein, Ioffe, and Larkin (Phys. Rev. B **55**, 3173 (1997)) for the underdoped spin-gap normal phase of the cuprates. A mean field approximation is derived which has many similarities to the numerical results. One difference however is an induced hole pairing in the odd-parity channel at arbitrary small dopings, similar to that proposed by Geshkenbein, Ioffe, and Larkin for the two-dimensional case. At higher dopings, we propose that a quantum phase transition will occur as holes enter the even-parity channels, resulting in a Luther-Emery liquid with hole pairing with essentially d-wave character. In the mean field approximation a crossover occurs which we interpret as a reflection of this quantum

phase transition deduced from the numerical results.

74.20.Mn,71.27.+a

I. INTRODUCTION

The properties of electrons confined to ladders with various numbers of legs have been investigated by many groups in the past few years [1]. The reason for this interest lies both in the unusual properties of the ladder systems and the possibility to realize ladder structures in the cuprates, but also in the insight these systems give to the full two-dimensional problem of a square lattice. Two different approaches have been taken. One is based on the weak-coupling limit and uses renormalization group methods to analyze the multi-leg ladders [2–7]. A very complete analysis of this type for N -leg ladders in the Hubbard model has recently been given by Lin, Balents and Fisher [7].

A second approach is more numerical and examines the strong-coupling limit described mostly by the t - J model. Recent progress on the loop algorithm for Monte Carlo calculations has allowed large undoped systems described by a Heisenberg model to be investigated down to very low temperatures. However, when doped holes are introduced, the fermion sign problem prevents one from using this method, and other methods must be employed, e.g. using Lanczos techniques to diagonalize relatively small systems [8,9] or the new density matrix renormalization group method (DMRG) to obtain the groundstate of large systems [10].

In this paper we examine the case of the lightly doped $t - J$ three-leg ladder. This case is specially interesting because in a certain sense it combines the contrasting properties of a single chain [11,12] and a two-leg ladder [8]. These behave quite differently, both when undoped or when lightly doped, so it is of great interest to follow the evolution of the three-leg ladder in this regime. In particular, the evolution of the Fermi surface as the Mott insulating state is approached is very different in the different transverse channels. As we shall discuss further below, this leads to a region where the Fermi surface is truncated in two channels, but remains in one channel - a behavior which clearly violates the Luttinger theorem. We shall argue that this presence of transverse channels which behave quite differently helps us to make inferences for the limit of the two-dimensional plane which of course can be

represented as the limit of very many channels or patches on the Fermi surface. The lightly doped limit of the three-leg ladder can serve as a simpler analog for the underdoped spin gap region of the cuprates, which has attracted so much attention, if one assumes that the patches or channels near $(\pm\pi, 0)$ and $(0, \pm\pi)$ are truncated and show a spin gap, while those near $(\pm\pi/2, \pm\pi/2)$ are gapless [13].

The t - J three-leg ladder Hamiltonian is given by

$$\begin{aligned}
H = & -t \sum_{j,\sigma} \sum_{\nu=1}^3 P(c_{j,\nu,\sigma}^\dagger c_{j+1,\nu,\sigma} + H.c.) P \\
& -t' \sum_{j,\sigma} \sum_{\nu=1}^2 P(c_{j,\nu,\sigma}^\dagger c_{j,\nu+1,\sigma} + H.c.) P \\
& + J \sum_j \sum_{\nu=1}^3 (\mathbf{S}_{j,\nu} \cdot \mathbf{S}_{j+1,\nu} - \frac{1}{4} n_{j,\nu} \cdot n_{j+1,\nu}) \\
& + J' \sum_j \sum_{\nu=1}^2 (\mathbf{S}_{j,\nu} \cdot \mathbf{S}_{j,\nu+1} - \frac{1}{4} n_{j,\nu} \cdot n_{j,\nu+1}), \tag{1}
\end{aligned}$$

where j runs over L rungs, $\sigma(=\uparrow, \downarrow)$, and ν are spin and leg indices. The t - J three-leg ladder is sketched in Fig. 1. The first two terms are the kinetic energy (P is a projection operator which prohibits double occupancy), and the last two exchange couplings J (J') act along the legs (rungs). Periodic or antiperiodic boundary conditions (PBC, APBC) are used along the legs.

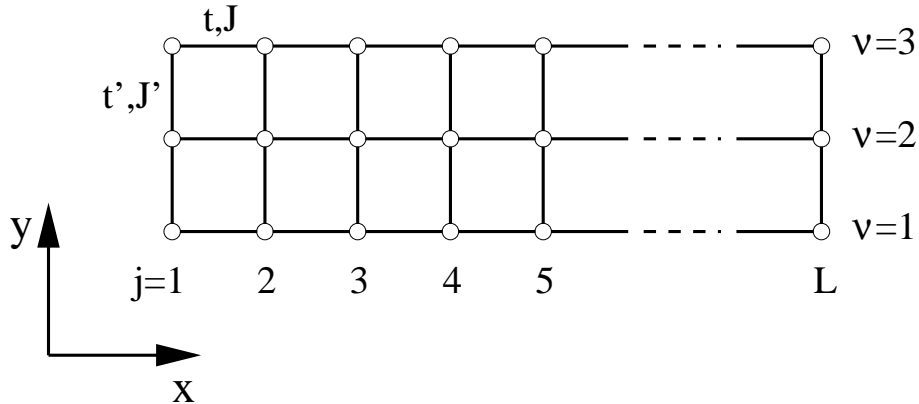


FIG. 1. The t - J ladder with three legs and L rungs. The couplings along the legs are t and J , and those along the rungs t' and J' .

The paper is organized as follows. In the next section we recapitulate briefly the known

results in the undoped limit described by a Heisenberg Hamiltonian. Then in section 3 we discuss the case of a single doped hole, using the results of a Lanczos diagonalization and also the earlier DMRG results by White and Scalapino [10]. The low-energy properties are described by a single Luttinger liquid channel in contact with an insulating spin liquid (ISL). Next in section 4 we consider states with two and more holes. In the presence of a finite hole density, there are two possibilities - either all the holes repel each other and enter the single Luttinger liquid channel, or at some density, the other channels are also populated with holes. Since doping a resonating valence bond (RVB) spin liquid leads to a Luther-Emery liquid [8], this will cause a qualitative change in the physical properties. There will be a critical hole density, δ_c , which controls the transition between the low-density phase with only a Luttinger liquid, in contact with a spin liquid, to the case with both Luttinger and Luther-Emery liquids. In section 5 we develop a mean field approach to the t - J three-leg ladder. In this mean field approximation, as we shall see, the critical density, δ_c , is not finite but arbitrarily small, whereas the numerical results give a finite δ_c for values of $J/t \sim 0.5$. In the final section we draw some conclusions and discuss the relationship to the planar two-dimensional case.

II. UNDOPED CASE: THE HEISENBERG THREE-LEG LADDER

In this section we recapitulate briefly the known results for three-leg ladders in the Heisenberg model. In this case the fermion sign problem does not occur, and very accurate quantum Monte Carlo calculations have been carried out by Frischmuth *et al.* [14], and by Greven *et al.* [15]. The low-energy properties can be mapped onto an effective single $S=1/2$ antiferromagnetic (AF) Heisenberg chain model, although the starting model has three spins per set of ladder rungs. This arises because the additional spin degrees of freedom have a spin gap, and enter with an excitation energy $\sim J'$. The spinon velocity of the effective model in fact is hardly changed from the value of the nearest neighbor Heisenberg chain with exchange constant J . However the energy scale parameter which controls the spinon-

spinon interactions and the size of logarithmic corrections to the uniform spin susceptibility at finite temperatures is greatly changed. Frischmuth *et al.* [14] interpret this result in terms of a Heisenberg model for the effective chain with longer range and unfrustrated effective interactions which act to enhance the AF correlations.

The key point however is the fact that the low-energy Hilbert subspace is greatly reduced so that not three chains but only a single chain model is active at low energies, or in other words only a single $S=1/2$ degree of freedom per rung of three spins remains in the low-energy region. The remaining spin degrees of freedom are gapped in the same way as the spin liquid of a two-leg ladder.

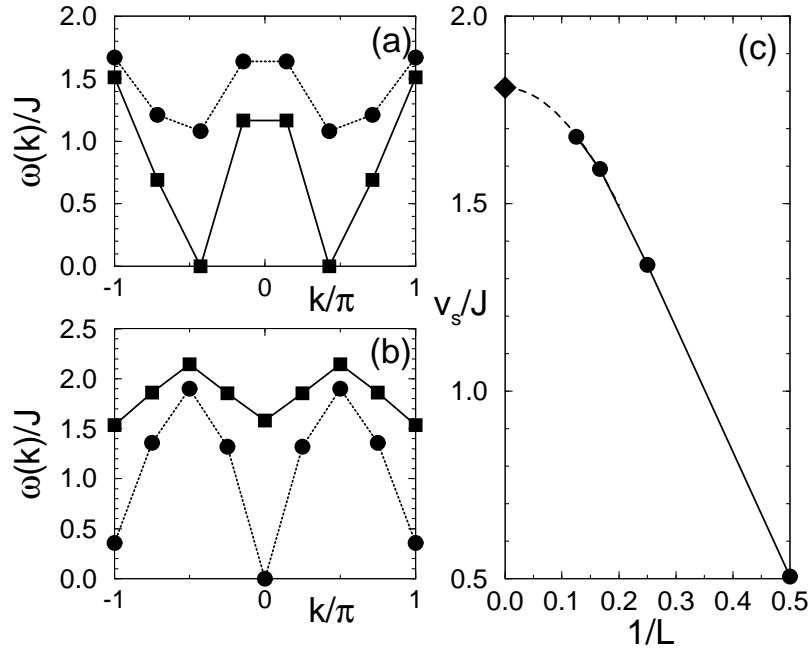


FIG. 2. (a) and (b) Spinon excitation spectra for the isotropic (3×7) - and (3×8) -site Heisenberg ladders. The circles correspond to the even parity and the squares to the odd parity channels respectively. (a) Single spinon excitation spectrum ($S = 1/2$) in a (3×7) -cluster. (b) Two-spinon excitation spectrum ($S = 1$) in a (3×8) -cluster. (c) Spinon-velocity, v_s , in $(3 \times L)$ -Heisenberg ladders. v_s extrapolates with high accuracy to the value 1.81J (diamond), obtained by QMC calculations [13].

This behavior is clearly observed in the numerical Lanczos diagonalization of (3×7) - and (3×8) -clusters, shown in Fig. 2. As Bares *et al.* [12] emphasized in their study of the exactly

solvable supersymmetric t - J model in one dimension, the spinon and holon dispersions can be directly obtained in the limit of vanishing hole density by examining the groundstate of an appropriately chosen finite chain. Thus if one takes the case of one undoped chain with an odd number of sites and PBC, then the groundstate for each total wavevector along the chain gives the dispersion of a single spinon. This groundstate manifold has a total spin quantum number $S=1/2$. For the present case of a three-leg ladder we show the dispersion for a (3×7) -sample with PBC in Fig. 2(a). The single spinon with $S=1/2$ has odd parity with respect to reflection about the center leg and disperses with a bandwidth $\sim \frac{\pi}{2}J$ and minima at $\pm\frac{\pi}{2}$. The corresponding one-spinon excitation spectrum of a 7-site single Heisenberg chain is shown in Fig. 3(a). To estimate finite size effects, the calculation was repeated for a 19-site Heisenberg chain (Fig. 3(c)). We observe that the qualitative features, i.e. the positions of extrema and the overall bandwidth, are already present in the smaller cluster. This is important since in the exact diagonalization study of $(3 \times L)$ -ladders, we are restricted to relatively small ($L \leq 8$) systems.

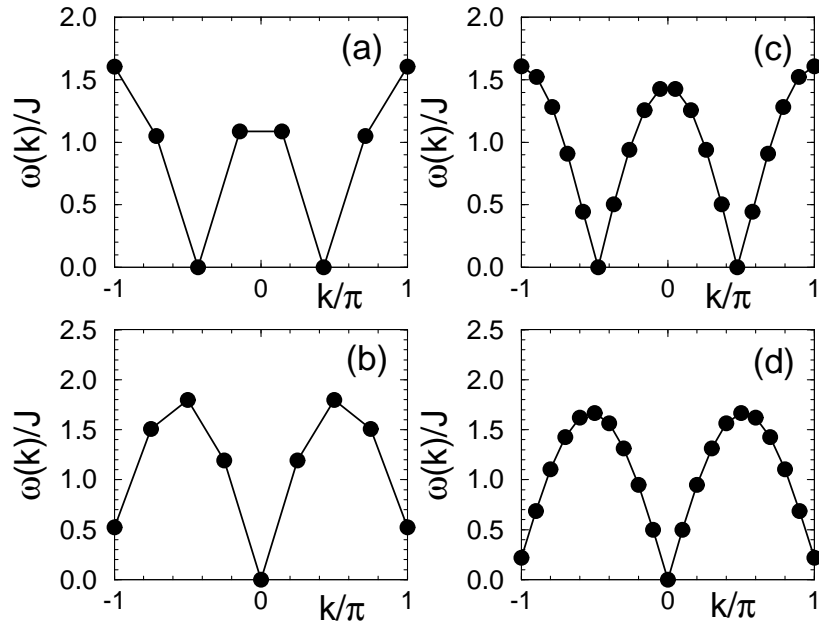


FIG. 3. Spinon excitation spectra for 7- and 8-site Heisenberg chains. (a) Single spinon excitation spectrum ($S = 1/2$) in a 7-site chain. (b) Two-spinon excitation spectrum ($S = 1$) in an 8-site chain. (c) Same as (a), but for a 19-site chain. (d) Same as (b), but for a 20-site chain.

For the (3×7) -ladder single spinon dispersion shown in Fig. 2(a), there appears an additional even-parity band, corresponding to the gapped spin degrees of freedom. It is separated from the odd-parity band by a gap $\sim J$, and its bandwidth is much smaller than that of the low-energy band. For the case of an even number of rungs (as shown in Fig. 2(b) for the case of (3×8)), the low-lying spin excitations now have even parity with respect to reflection about the center leg, and involve pairs of spinons with $S=1$ and groundstate wavevectors $k=\pm\frac{\pi}{2}\pm\frac{\pi}{2}=0,\pm\pi$. The finite size gap at $k=\pm\pi$ vanishes in the thermodynamic limit. Again, a comparison of the low-energy two-spinon band with that of the corresponding 8-site single Heisenberg chain (Fig. 3(c)) shows qualitative (almost quantitative) agreement, supporting our conclusion that the low-energy degrees of freedom of the $(3 \times L)$ -ladders can be mapped onto effective single chains.

Finally, we analyze the finite size scaling behavior of the spinon velocity, $v_s = \frac{\partial\omega}{\partial k}|_{k=0}$, for the three-leg Heisenberg ladders (Fig. 2(c)). In the finite systems, we approximate the derivative by $v_s \approx \frac{\omega(2\pi/L)-\omega(0)}{2\pi/L}$ (L even). Using $L=2, 4, 6$, and 8 , we obtain with the approximate scaling form, $v_s(L) = v_s(\infty) + aL^{-2} + bL^{-4}$, a bulk value of $v_s(\infty) \simeq 1.81J$, which is in excellent agreement ($\sim 1\%$) with that obtained by recent QMC calculations on clusters with up to 600 spins [16].

III. SINGLE HOLE IN A THREE-LEG LADDER

We start the study of effects of doping by recalling the single electron non-interacting bandstructure. This takes the form of three overlapping bands (in the isotropic case $t = t'$). These can be classified according to their parity under the reflection operation (R) about the center leg. The two even-parity bands we denote as bonding (b) and anti-bonding (ab), and they have the dispersion relation

$$\epsilon_{b,ab}(k) = \mp\sqrt{2}t' - 2t \cos k, \quad (2)$$

while the odd-parity band (or non-bonding band) has the form

$$\epsilon_{nb}(k) = -2t \cos k. \quad (3)$$

At half-filling, the chemical potential is $\mu = 0$, and all three bands are partially filled. The Fermi surface consists of three pairs of Fermi points $(\pm k_{F,\lambda}, \lambda = ab, nb, b)$, arising from each band (or channel).

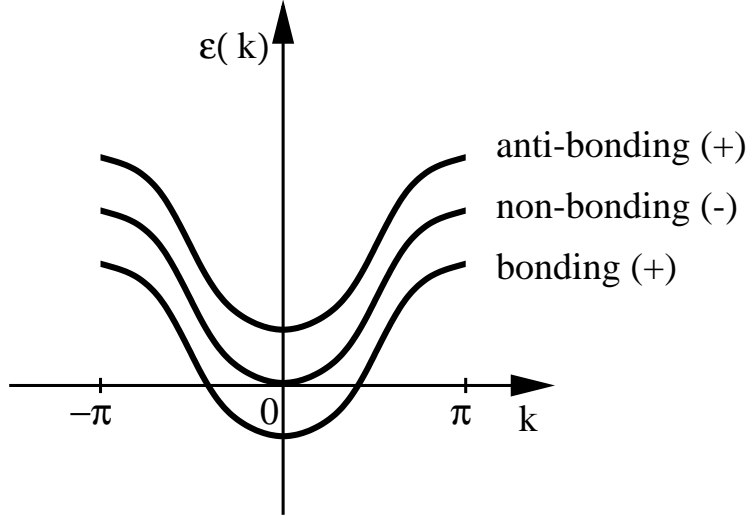


FIG. 4. Schematic plot of the non-interacting one-electron bandstructure of a $(3 \times L)$ -ladder. The parities of the bands with respect to reflection about the center leg are indicated by (\pm) . The splitting between the bands is $\sqrt{2}t'$.

We consider the case of a single hole, and we start with a (3×7) -sample. The groundstate is now a total singlet ($S=0$) and non-degenerate. The wavevector dependence determines the single holon dispersion, again in a single chain effective model. In Fig. 5(a), the results are shown for a parameter value $J/t = 0.5$. The holon energy has absolute minima at $k=\pm\pi$ and a local minimum at $k=0$. This latter behavior is consistent with a finite size effect. For example in Fig. 5(c) we show the holon dispersion calculated in a 7-site single chain $t - J$ model where a similar behavior is obtained. This in turn reflects the doubling of the period in the single Heisenberg chain dispersion, when the chain length goes to infinity.

The three-leg ladder has reflection symmetry with respect to the center leg. The eigenvalues of the corresponding operator, R , are ± 1 , i.e. even (odd) parity under reflection. The groundstate for the undoped ladder with $(3 \times L)$ legs (L odd) has parity -1. The groundstate

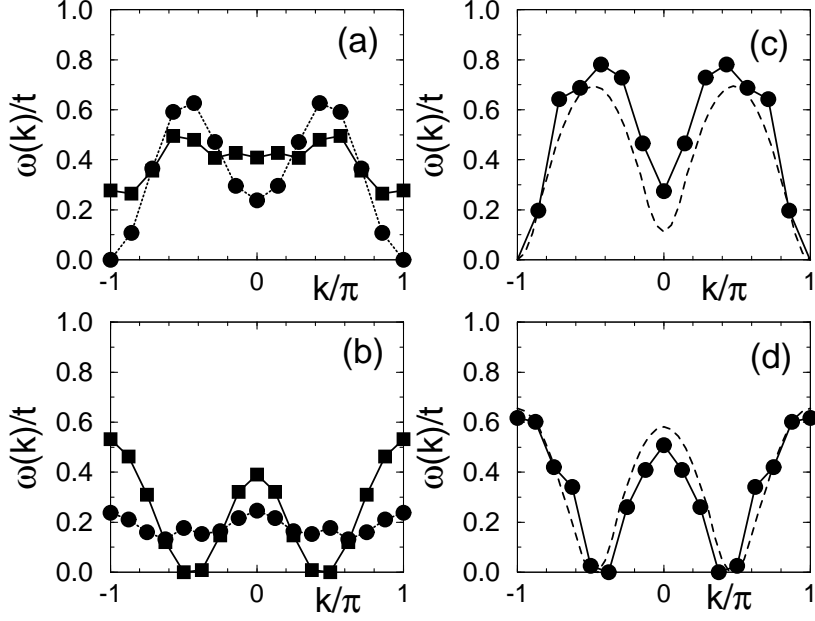


FIG. 5. Hole excitation spectra for the isotropic (3×7) - and (3×8) -site $t - J$ ladders, and for 7- and 8-site $t - J$ chains. In (a) and (b), the circles correspond to the even parity and the squares to the odd-parity channels respectively. (a) Single holon ($\delta = 1/21$, $S = 0$) in a (3×7) -cluster. (b) Single hole excitation spectrum ($\delta = 1/24$, $S = 1/2$) in a (3×8) -cluster. (c) Filled circles: single holon excitation spectrum ($\delta = 1/21$, $S = 0$) in a 7-site chain. Dashed line: same in a 19-site chain. (d) Filled circles: single hole excitation spectrum ($\delta = 1/24$, $S = 1/2$) in an 8-site chain. Dashed line: same in a 20-site chain.

manifold of the same ladders with one hole has parity $+1$. Therefore we associate parities $+1$ and -1 with a single holon and spinon respectively. It follows that the parity of a single hole which is the product of those parities is -1 , i.e. the hole goes into the band with odd parity with respect to R . This is the middle non-bonding band with odd parity. The interpretation is clear: the two bands with even parity in the $t - J$ model combine to form a spin liquid which is insulating (ISL), and the initial doped holes go into the odd-parity band (or channel), and form a single Luttinger liquid (LL). So the non-interacting bandstructure Fermi surface is truncated from three sets of Fermi points to a single Luttinger liquid in the odd channel. Note that this Fermi surface truncation implies a form of spin pairing and a reduction of the low-energy spin degrees of freedom, but it does not imply the formation of

Cooper pairs. Note also that this Fermi surface truncation is not due to a breaking of translational symmetry along the ladder since the spin-spin correlations in the ISL are purely short ranged.

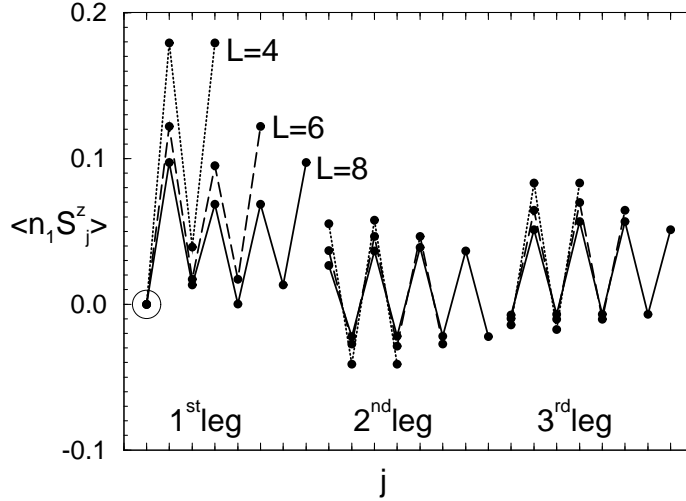


FIG. 6. Spin-charge correlations for one hole in $(3 \times L)$ isotropic $t - J$ clusters with $L = 4, 6, 8$, and $J/t = 0.5$. The holon is fixed at the site indicated by the circle.

White and Scalapino have performed DMRG calculations on large samples (3×16) with open boundary conditions [10]. They find upon doping a single hole that the spin and charge densities are well separated, indicating the decay of a single hole into a separated spinon and holon as expected for a Luttinger liquid. The Lanczos results for smaller clusters show similar results. In Fig. 6, the results for the spin-charge correlation are shown. If we add one hole to a $(3 \times L)$ cluster with L even, then the groundstate has total spin $S=1/2$, and odd parity. Therefore if we take the state with $S^z = +1/2$, we can calculate the local value of S^z at each site for configurations with the holon fixed at the origin. In Fig. 6, we show these results for $L=4, 6$, and 8 . The results show clearly that the spin is distributed over the whole cluster, and agree nicely with those of White and Scalapino [10]. This behavior is fully consistent with a single Luttinger liquid interpretation.

The Lanczos method allows one to examine also the low-lying excited states. This in turn raises the question of the energy gap between the Luttinger liquid with odd parity and the

TABLE I. Energies (in units of t) of the (3×6) -site isotropic $t - J$ ladder with antiperiodic boundary conditions and $J/t = 0.5$.

0 holes			1 hole			2 holes		
k	R	energy	k	R	energy	k	R	energy
0	+1	-9.017603	$\pi/6$	+1	-10.24582	0	+1	-11.80680
$\pi/3$	+1	-8.393170	$\pi/2$	+1	-10.25131	$\pi/3$	+1	-11.42219
$2\pi/3$	+1	-8.409188	$5\pi/6$	+1	-10.25673	$2\pi/3$	+1	-11.49704
π	+1	-9.243230				π	+1	-11.69586
0	-1	-8.450508	$\pi/6$	-1	-9.987594	0	-1	-11.59084
$\pi/3$	-1	-8.211651	$\pi/2$	-1	-10.40757	$\pi/3$	-1	-11.57428
$2\pi/3$	-1	-8.224553	$5\pi/6$	-1	-10.18534	$2\pi/3$	-1	-11.53402
π	-1	-8.403831				π	-1	-11.54535

next channel with even parity. This latter channel should correspond to placing the hole in the spin liquid. From the experience with the two-leg ladder one expects that doping the spin liquid will lead to a Luther-Emery liquid with a bound spin-charge distribution for a single hole. Therefore if our expectation is correct, we should expect the lowest-lying excited states with even parity to show a very different spin-charge distribution. In Fig. 7, we show the corresponding distributions for the lowest eigenstates with even and odd parities of clusters with $L=6$. The eigenvalues are given in Table 1. The difference is clear. In the odd parity channel the energy dispersion is large, the minimum energy lies at $k=\pm\pi/2$, corresponding to a half-filled Luttinger liquid. In the even parity channel, the energy dispersion is much less, and the minimum lies at values $k=\pm5\pi/6$ which we interpret as a hole entering the anti-bonding even parity band. As can be seen from Fig. 7, the instantaneous spin-charge distribution for this minimum energy even parity state is quite different, and shows a clear binding of the spin and charge. This behavior is fully consistent with that of a single hole in a Luther-Emery liquid and with the interpretation of a spin liquid in the even parity

channels. Also shown in Fig. 7 are the instantaneous spin-charge distributions for the set of lowest excited states with fixed wavevector and parity. These show intermediate behavior which we interpret as arising from (attractive) interactions between a spinon and a holon at wavevectors away from the Fermi surface.

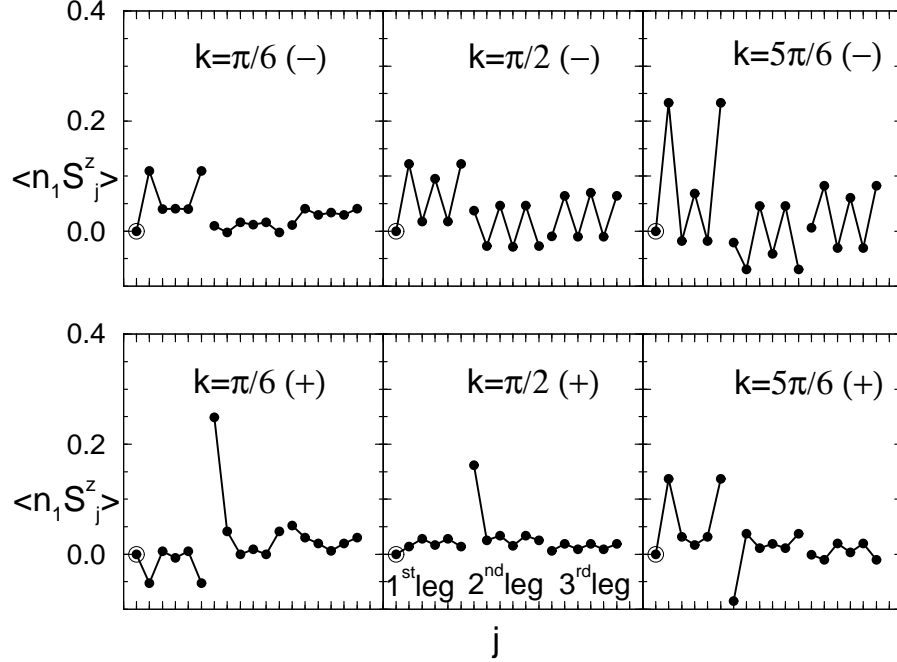


FIG. 7. Spin-charge correlations for one hole in a (3×6) -site isotropic $t - J$ cluster with $J/t = 0.5$. The holon is fixed at the site indicated by the circle.

An important quantity is the single hole energy gap between the odd and even parity channels. The value we obtain in the (3×6) -cluster is $\approx 0.15t$ (or $0.30J$) - a value which is smaller than that of the spin gap in the ISL ($\approx J$).

To summarize, the results for a single hole show that the minimum energy is in the non-bonding channel, and this channel forms a single Luttinger liquid. The even channels are gapped, forming an insulating spin liquid (ISL), and the minimum energy for a single hole in these channels lies higher in energy.

IV. TWO AND MORE HOLES

We begin with the case of two holes. White and Scalapino have performed DMRG calculations for $(3 \times L)$ -samples with a value of $J/t = 0.5$ [10]. They find that the holes do not bind and in fact repel each other, so that the most likely configuration has the two holons as widely separated as possible, consistent with the open boundary conditions used in their study. This behavior can be immediately interpreted as that of two holes doped in a single Luttinger liquid (LL), while the remaining transverse channels form an ISL, consistent with the discussion given above. In view of the finite energy gap between the even and the odd parity states, there will be a finite density range within which this LL + ISL phase remains stable. We then conclude that the hole density in the White-Scalapino calculations ($\delta = 1/24$) lies within this density range.

The next issue is to determine the critical hole density, δ_c , that limits the stability of this LL + ISL phase. At first sight it would seem straightforward to use the single hole energy gap between odd and even parities to determine the critical value for the hole chemical potential, μ_c , and thus δ_c : $\mu_c = \mu(\delta_c)$. However, we expect the even parity channels to evolve into a Luther-Emery liquid (LE) when doped, in analogy to the doped two-leg ladder. As a result, μ_c will be determined by the energy of the two-hole bound state of the LE rather than the single-hole energy gap.

In Fig. 8, we show the instantaneous hole-hole correlation function for various two-hole states of a (3×6) -cluster with APBC ($J/t=0.5$). These boundary conditions were chosen since they give a non-degenerate (i.e. closed shell) groundstate for non-interacting electrons [17]. The groundstate has even parity and a total wavevector of $k=0$. The instantaneous hole-hole correlation function (Fig. 8(a)) shows the maximum weight at the largest rung-rung separation possible in this small cluster, but with both holes preferentially on the same edge. This behavior is similar to that found by White and Scalapino, and leads us to interpret this as a groundstate with LL + ISL character. Note that the hole density here ($\delta = 1/9$), is larger than that considered by White and Scalapino.

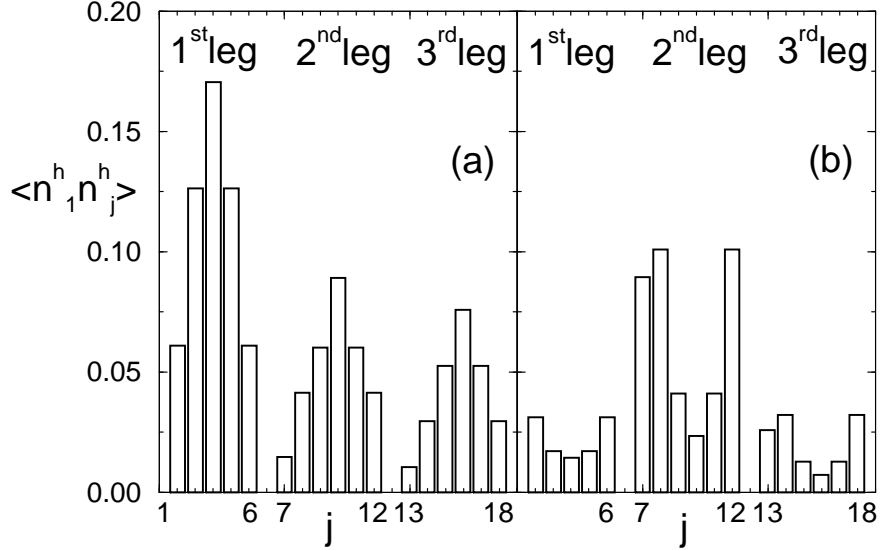


FIG. 8. Instantaneous hole-hole correlations for two holes in a (3×6) -site isotropic $t - J$ cluster with $J/t = 0.5$. The first hole is fixed at the origin ($j=1$), not shown in the figure. (a) groundstate, $k=0$. (b) excited state, $k=\pi$. The sites on the first (outer) leg are labeled $1 \leq j \leq 6$, on the second (center) leg $7 \leq j \leq 12$, and on the third (outer) leg $13 \leq j \leq 18$.

There should however be an excited state of the cluster, also with even parity and $S=0$, which has the two holes in the LE. This state should have a total wavevector of $k = \pi$, i.e. the same value as the undoped system [18]. In fact, such a state appears in the cluster with an excitation energy of $0.111t$ above the groundstate. The instantaneous hole-hole correlations in this excited state (Fig. 8(b)) are also quite different from the groundstate, with a maximum for the next-nearest-neighbor separation, indicating that the two holes are bound in this state. Therefore we identify this state as that with two holes in a LE formed from the even parity transverse channels (i.e. bonding and anti-bonding bands). This identification is confirmed if we look at the average hole density on the central vs. the outer legs. The results quoted in Table 2 show a marked increase in the hole density on the central leg in the LE state.

The binding energy of the two holes in the LE state can be estimated from the energy

TABLE II. Average hole densities on the central and the outer legs in the (3×6) -site isotropic $t - J$ ladder with two holes and $J/t = 0.5$.

k	R	$\langle n^h \rangle_{\text{out}}$	$\langle n^h \rangle_{\text{central}}$
0	+1	1.050053	0.899894
$\pi/3$	+1	0.791384	1.417232
$2\pi/3$	+1	0.809848	1.380304
π	+1	0.794342	1.411316
0	-1	1.170123	0.659754
$\pi/3$	-1	0.995565	1.00887
$2\pi/3$	-1	0.978532	1.042936
π	-1	0.884392	1.231216

difference to add the two holes *together* in the LE state (E_2^{LE}) and *separately* in the LE state (E_1^{LE}). This difference is an estimate of the binding energy, $E_b = 2E_1^{\text{LE}} - E_2^{\text{LE}} = -2.028t + 2.453t = 0.425t$. Note however that this value may well be a considerable overestimate because of finite size effects (see below).

We now turn to the estimate of the chemical potential, $\mu(\delta)$. In view of the small size of the clusters (i.e. mostly 3×6 sites) we need to take care about finite size corrections. In particular, in small clusters there is generally a large energy gain for total singlet states, and if one calculates μ through single hole additions one ends up subtracting the energies of states with total spin $S=0$ and $S=1/2$. In order to avoid this, we use two-hole additions since then the total spin quantum number remains unchanged; i.e. $\mu(\delta) = \frac{1}{2}[E_G(N_h + 1) - E_G(N_h - 1)]$. The result is shown in Fig. 9. The curve of $\mu(\delta)$ rises initially with δ , consistent with a repulsive interaction between holes in the LL + ISL phase. Our previous estimate of the excitation energy of the LE state with $N_h = 2$ allows us to determine the chemical potential rise needed for holes to enter the LE phase at $0.055t$. From Fig. 9 we estimate then for the critical hole density a value of $\delta_c \simeq 0.13$. Note that this value is calculated using a relatively

small cluster size, and it is not possible to estimate the finite size corrections. Therefore this value of δ_c is an estimate whose accuracy is hard to predict.

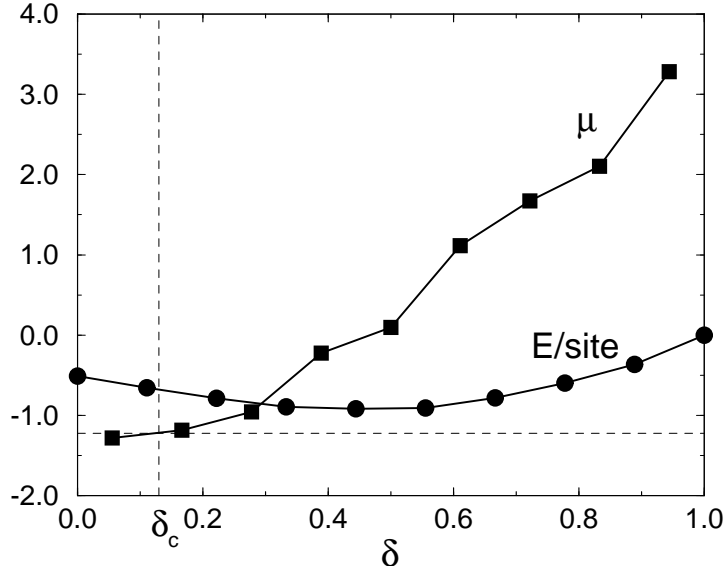


FIG. 9. Energy per site (circles) and chemical potential (squares) for a (3×6) -site isotropic $t-J$ ladder with $J/t=0.5$. The critical hole density, δ_c , beyond which the holes enter the LE phase is indicated by a dashed line.

We conclude that the LL + ISL phase remains stable over a finite hole density range, $0 < \delta < \delta_c$, and in this range there is no hole pairing although a large fraction of the spin degrees of freedom are gapped in the ISL. Beyond this density range, $\delta > \delta_c$, there is a LE channel in contact with the LL channel. The presence of holes in a LE channel leads to hole pairing and dominant superconducting or charge density wave correlations as in the case of the lightly doped two-leg ladder.

In order to further explore the low-density LL + ISL phase, we calculated the single particle spectral function, $A_\lambda(k, \omega) = -\frac{1}{\pi} \text{Im}[G_\lambda(k, \omega - i\eta)]$, in the groundstate of the (3×6) -cluster with two holes. Here, λ labels the linear combinations of c-operators, corresponding to the non-interacting shell structure shown in Fig. 5: $c_{j,b,\sigma} = \frac{1}{2}[c_{j,1,\sigma} + \sqrt{2}c_{j,2,\sigma} + c_{j,3,\sigma}]$, $c_{j,nb,\sigma} = \frac{1}{\sqrt{2}}[c_{j,1,\sigma} - c_{j,3,\sigma}]$, $c_{j,ab,\sigma} = \frac{1}{2}[c_{j,1,\sigma} - \sqrt{2}c_{j,2,\sigma} + c_{j,3,\sigma}]$. The results are displayed in Fig.

10 for (3×6) ladders with APBC and PBC. The energy region below the chemical potential corresponds to a transition to three-hole states. In a small cluster, such as the (3×6) under study here, the finite size effects are large. Thus to interpret the spectrum, one should keep in mind the non-interacting shell structure. We begin with the case of APBC. The two-hole LL + ISL state has then 16 electrons which in a non-interacting state would occupy the states $b(\pm\frac{\pi}{6}, \pm\frac{\pi}{2})$, $ab(\pm\frac{\pi}{6})$, and $nb(\pm\frac{\pi}{6})$. Through the strong correlation interaction the state with electron pairs in the $b(\pm\frac{5\pi}{6})$ state will be admixed. In this way we can interpret the electron removal (or photoemission) part of the spectrum with the strong peaks to inserting holes into the $b(\pm\frac{\pi}{2}, \pm\frac{5\pi}{6})$ and $ab(\pm\frac{\pi}{6})$ even parity channels. The state with an added hole at $b(\pm\frac{\pi}{6})$ is far removed from the Fermi level, and so it is strongly broadened. Turning to the nb -channel, we see that the main weight is at $(\pm\frac{\pi}{6})$ as expected, but this is again broadened due to many-body effects. The resulting photoemission spectrum then shows signs of a Fermi surface in all three channels, and with k_F -values in line with our expectations.

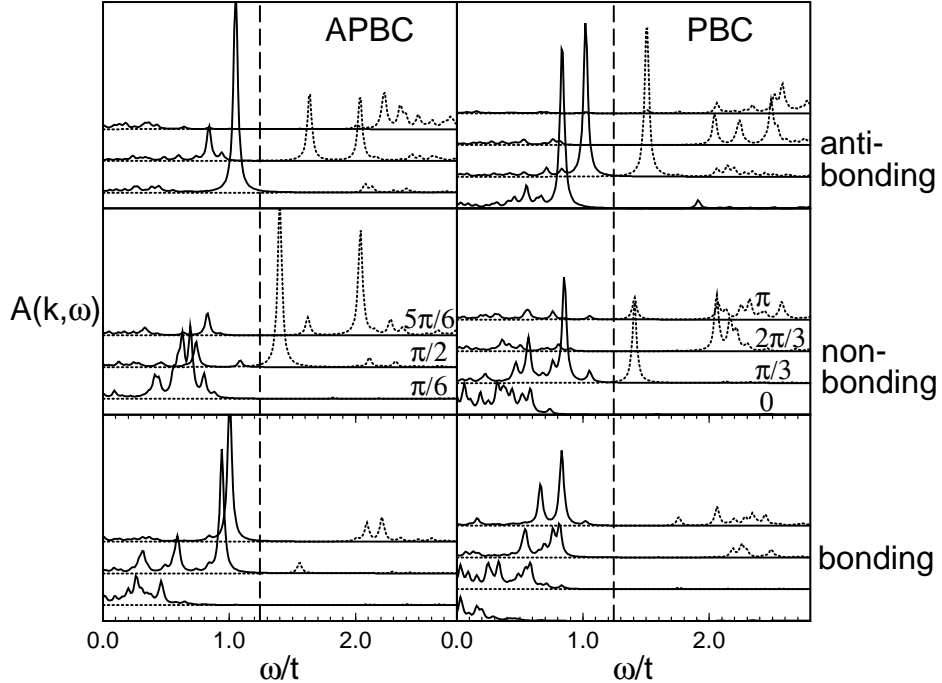


FIG. 10. Spectral functions for a (3×6) -site isotropic $t - J$ ladder with two holes and $J/t=0.5$. The poles have been given a finite width of $\eta = 0.02t$, and the chemical potential is indicated by the dashed line. APBC (PBC) were used in the left (right) panel.

Clearly all three bands (b , ab , and nb) are partially occupied. This is illustrated by calculating the momentum distribution function, $n_\lambda(k) = \int^\mu d\omega A_\lambda(k, \omega)$. The results for $n_\lambda(k)$ are shown in Fig. 11. These show drops as k increases which one can interpret as giving estimates for $k_{F,\lambda}$, but in a small system one cannot draw conclusions about the actual behavior for $k \sim k_{F,\lambda}$. The case of PBC has a different shell structure. The LL + ISL state is now a state with total momentum $\pm 2\pi/3$, with the 4 electrons in the nb -channel occupying $k=0$ (2 electrons) and $k=\pm\pi/3$ (2 electrons) [19]. The values of $n_\lambda(k)$ for PBC in the LL + ISL state are also included in Fig. 11, and also confirm the interpretation of a partial filling of all three bands.

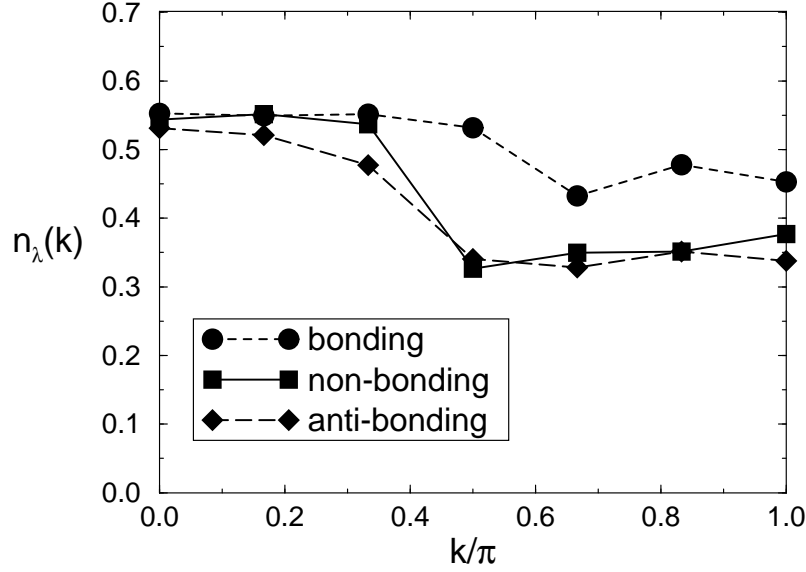


FIG. 11. Momentum distribution function for a (3×6) -site isotropic $t - J$ ladder with two holes and $J/t=0.5$. Results with APBC and PBC were combined.

However, at a true Fermi surface in a bulk system one must be able to *add* as well as to remove electrons at the chemical potential (or Fermi energy). The strong correlation condition clearly influences this part of the spectrum much more strongly, since as we pass to the undoped Mott insulator electron addition is totally forbidden (or allowed only on paying the Mott correlation energy gap), whereas in photoemission electrons can always be

removed. With this in mind we examine the electron addition part of the spectrum which corresponds to a transition to a one-hole state. From Fig. 10 we see that the main weight at low energy is in the $nb(\pm\frac{\pi}{2})$ -channel. Clearly this corresponds to a transition from the two-hole LL + ISL-groundstate to the one-hole LL + ISL-groundstate, and confirms that we have a Fermi surface in the odd-parity LL-channel. Next we look at the even-parity channels which form an ISL in the groundstate. Therefore we should expect that then electron addition in these channels at low energy will be forbidden. In fact, if we look at the b -channel, then this behavior is clear, and there is no Fermi surface in this channel. On the other hand, in the other even-parity channel, $\lambda = ab$, we find two relatively strong peaks at $k = \pm\frac{\pi}{2}$. These values actually correspond to a transition not to the minimum energy state of one hole in this channel but to an excited state. We interpret these peaks as sidebands, involving the creation of a S=1 odd-parity magnon with $k = 0$ or π in addition. Clearly it is too strong a statement to say that all processes which add an electron to a LL + ISL-state with even parity are forbidden, since sidebands in which an electron is added in the odd-parity LL channel and simultaneously odd-parity S=1 magnons are created can have a total parity which is even and a total spin of S=1/2. We interpret the weight in the ab -channels then in terms of such processes which in turn may be enhanced by the finite size effects associated with these small clusters. The behavior of the PBC case is analogous. Here the main weight at low energy is the nb ($k=\pi/3$) channel, corresponding also to a transition to the one-hole LL + ISL state. However, again there is weight in the antibonding channel which we interpret also as a higher energy sideband and a transition to a one-hole LE state. This is strongly admixed due to the enhanced stability of this state which has a filled shell character in the nb -channel as we discussed earlier.

In conclusion, the single particle spectra in the LL + ISL state show a strong asymmetry between removing and adding electrons, and it is the latter process, which unfortunately is not easy to detect experimentally, where the effects of the Fermi surface truncation on approaching the Mott insulating state are most evident.

V. ANALYSIS BY MEAN FIELD THEORY

In this section we analyze the properties of the three-leg ladder using the mean field description in the same spirit as previously done for the two-leg ladder [20]. For this purpose we introduce spinon and holon operators, f and b respectively, by replacing the electron creation and annihilation operators in the following way [21],

$$c_{i,\nu,\sigma}^\dagger = f_{i,\nu,\sigma}^\dagger b_{i,\nu} \quad \text{and} \quad c_{i,\nu,\sigma} = b_{i,\nu}^\dagger f_{i,\nu,\sigma} \quad (4)$$

which lead to the local constraint $\sum_\sigma f_{i,\nu,\sigma}^\dagger f_{i,\nu,\sigma} + b_{i,\nu}^\dagger b_{i,\nu} = 1$. The Hamiltonian can be reformulated in these operators, and can then be decoupled by introducing mean fields. The constraint is included by adding a term with Lagrange multipliers. Since this treatment is quite standard we do not go into details here. The system is not translationally invariant along the rung, so that the mean fields depend on the position of the bonds, resulting in 10 independent mean fields: 6 hopping and 3 pairing mean fields, defined on nearest neighbor bonds $(j, \nu; j', \nu')$,

$$\begin{aligned} \chi_{j,\nu;j',\nu'} &= \frac{1}{2} \sum_\sigma \langle f_{j,\nu,\sigma}^\dagger f_{j',\nu',\sigma} \rangle \\ B_{j,\nu;j',\nu'} &= \langle b_{j,\nu} b_{j',\nu'}^\dagger \rangle \end{aligned} \quad (5)$$

$$\Delta_{j,\nu;j',\nu'} = \langle f_{j,\nu\downarrow} f_{j',\nu'\uparrow} \rangle$$

and a uniform Lagrange multiplier μ . We denote the mean fields along the outer two legs and the middle leg with the index 1 and 2, respectively, while the rung mean fields have the index 3. In order to avoid ambiguities we have to define the direction of the bond mean fields. We give here the convention using the example of χ ,

$$\chi_1 = \frac{1}{2} \sum_{\sigma} \langle f_{j,\nu,\sigma}^{\dagger} f_{j+1,\nu,\sigma} \rangle \quad \nu = 1, 3$$

$$\chi_2 = \frac{1}{2} \sum_{\sigma} \langle f_{j,2,\sigma}^{\dagger} f_{j+1,2,\sigma} \rangle \quad (6)$$

$$\chi_3 = \frac{1}{2} \sum_{\sigma} \langle f_{j,2,\sigma}^{\dagger} f_{j,\nu,\sigma} \rangle \quad \nu = 1, 3$$

The same convention is applied to the mean fields B and Δ . The parity with respect to the reflection operator R allows us to separate the mean field Hamiltonian into the even (+) and odd (−) parity channels,

$$\begin{aligned} H_{\text{mf}} = & H_+^{(b)} + H_-^{(b)} + H_+^{(f)} + H_-^{(f)} \\ & + L[\mu + \frac{J}{2}(2\chi_1^2 + \chi_2^2 + 2\Delta_1^2 + \Delta_2^2) + J'(\chi_3^2 + \Delta_3^2) \\ & + 2t(B_1\chi_1 + B_2\chi_2) + 4t'B_3\chi_3] \end{aligned} \quad (7)$$

We define the corresponding combinations for the operators, operator combinations,

$$\begin{aligned} f_{k\pm,\sigma} &= \sqrt{\frac{1}{2L}} \sum_j (f_{j,1,\sigma} \pm f_{j,3,\sigma}) e^{ikr_j} \\ b_{k\pm} &= \sqrt{\frac{1}{2L}} \sum_j (b_{j,1} \pm b_{j,3}) e^{ikr_j} \end{aligned} \quad (8)$$

with the momentum k along the legs of the ladder. Then we can write the four terms of the Hamiltonian (in Nambu space for the spinons) as

$$H_-^{(b)} = (-4t\chi_1 \cos k - \mu)b_{k-}^\dagger b_{k-}$$

$$H_+^{(b)} = (b_{k+}^\dagger, b_{k,2}^\dagger) \begin{bmatrix} -4t\chi_1 \cos k - \mu & -2\sqrt{2}t'\chi_3 \\ -2\sqrt{2}t'\chi_3 & -4t\chi_2 \cos k - \mu \end{bmatrix} \begin{pmatrix} b_{k+} \\ b_{k,2} \end{pmatrix}$$

$$H_-^{(f)} = \sum_\sigma (f_{k-, \sigma}^\dagger, f_{-k-, -\sigma}) \begin{bmatrix} -(2tB_1 + \frac{3}{2}J\chi_1) \cos k - \mu & -\frac{3}{2}J\Delta_1 \cos k \\ -\frac{3}{2}J\Delta_1 \cos k & (2tB_1 + \frac{3}{2}J\chi_1) \cos k + \mu \end{bmatrix} \begin{pmatrix} f_{k-, \sigma} \\ f_{-k-, -\sigma}^\dagger \end{pmatrix}$$

$$H_+^{(f)} = (f_{k+\uparrow}^\dagger, f_{k,2,\uparrow}^\dagger, f_{-k+\downarrow}, f_{-k,2,\downarrow}) \begin{bmatrix} \hat{\xi}_k & \hat{\Delta}_k \\ \hat{\Delta}_k & -\hat{\xi}_{-k} \end{bmatrix} \begin{pmatrix} f_{k+\uparrow} \\ f_{k,2,\uparrow} \\ f_{-k+\downarrow}^\dagger \\ f_{-k,2,\downarrow}^\dagger \end{pmatrix} \quad (9)$$

where $\hat{\xi}_k$ and $\hat{\Delta}_k$ are 2×2 -matrices of the form

$$\hat{\xi}_k = \begin{bmatrix} -(2tB_1 + \frac{3}{2}J\chi_1) \cos k - \mu & -2\sqrt{2}t'B_3 - \frac{3\sqrt{2}}{4}J'\chi_3 \\ -2\sqrt{2}t'B_3 - \frac{3\sqrt{2}}{4}J'\chi_3 & -(2tB_2 + \frac{3}{2}J\chi_2) \cos k - \mu \end{bmatrix} \quad (10)$$

$$\hat{\Delta}_k = \begin{bmatrix} -\frac{3}{2}J\Delta_1 \cos k & -\frac{3\sqrt{2}}{4}J'\Delta_3 \\ -\frac{3\sqrt{2}}{4}J'\Delta_3 & -\frac{3}{2}J\Delta_2 \cos k \end{bmatrix}$$

Note that we have neglected the terms with $-n_i n_j / 4$ in the exchange term, because in the mean field calculation they tend to artificially enhance the tendency towards pairing and favor a flux phase close to half-filling.

We can now solve the single-particle problem of H_{mf} and determine the mean fields self-consistently. For the groundstate we obtain the self-consistent equations by minimizing the groundstate energy of H_{mf} in Eq.(4) with respect to all mean fields. In this description the

holons are Bose-condensed so that $\sum_{\nu=1,2,3} \langle b_{j,\nu}^\dagger b_{j,\nu} \rangle = 3\delta$ where δ is the doping concentration. In the following, we will use the same parameters as used in the numerical simulations, $t = t' = 2J = 2J'$.

A. Half filling

For half-filling, $\delta = 0$, there are no holons and the Hamiltonian of the spinons is invariant under the following SU(2) transformation

$$\begin{pmatrix} f_{j,\nu,\sigma}^\dagger \\ f_{j,\nu,-\sigma} \end{pmatrix} \rightarrow \hat{U} \begin{pmatrix} f_{j,\nu,\sigma}^\dagger \\ f_{j,\nu,-\sigma} \end{pmatrix} = \begin{pmatrix} f_{j,\nu,\sigma}'^\dagger \\ f_{j,\nu,-\sigma}' \end{pmatrix} \quad (11)$$

which reflects the constraint at half-filling. The absence of an up-spin corresponds to the presence of a down-spin and vice versa [22]. Note that due to the SU(2) invariance of the Hamiltonian the self-consistent solution of the mean field is not unique, but \hat{U} corresponds to a rotation in the mean field space $\{\chi_{1,2,3}, \Delta_{1,2,3}\}$ which leaves the groundstate and the excitation spectrum unchanged.

In this formulation various properties of the three-leg ladder can be interpreted at least on a qualitative level. The Hamiltonian yields six distinct bands in Nambu space for the spinons (Fig. 12). For the symmetric channel the spinons have a gapped spectrum where the lower two bands are completely filled. On the other hand, the antisymmetric channel has gapless excitations which give a spectrum analogous to that of a single chain. It is now easy to compare the spin excitation spectrum of the mean field and the exact diagonalization. For the mean field case the excitation corresponds to a particle-hole excitation of the spinon gas. The gapless spectrum is that of a single Heisenberg chain and is exactly what we obtain for the same type of mean field treatment of a single chain. The other bands are gapped and describe a spin liquid state coexisting with the gapless system. The agreement with the numerical simulation is qualitatively very good.

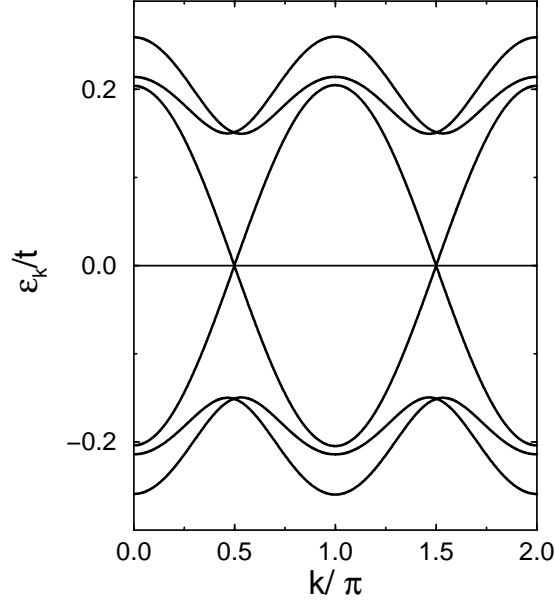


FIG. 12. Spinon bands at half filling obtained by the mean field theory. All states below the chemical potential (located at $\epsilon_k = 0$) are occupied by a spin-up and a spin-down spinon. The gapped bands correspond to the even-parity states, while the gapless bands in the center are in the odd-parity channel.

B. A single hole

We now insert a single hole into the half-filled system, i.e. we remove one spinon and add one holon. This immediately breaks the $SU(2)$ symmetry, because the groundstate energy of the holon has to be minimized which yields a constraint on the hopping mean fields χ_i . Three holon bands appear, two even parity bands and one odd parity band, with energies given by

$$\begin{aligned}
 \epsilon_{k+} &= -2t(\chi_1 + \chi_2) \cos k - \mu \\
 &\quad \pm \sqrt{4t^2(\chi_1 - \chi_2)^2 \cos^2 k + 8t^2\chi_3^2} \\
 \epsilon_{k-} &= -4t\chi_1 \cos k - \mu.
 \end{aligned} \tag{12}$$

Obviously the lowest holon state can be found in the lower of the two even-parity bands. Thus, the single hole groundstate can be obtained by removing a spinon at the Fermi level of the odd-parity band and by inserting a holon at bottom of the lower even-parity holon band. This results in a change of the parity of the groundstate compared with that of the half-filled case, in agreement with the numerical result.

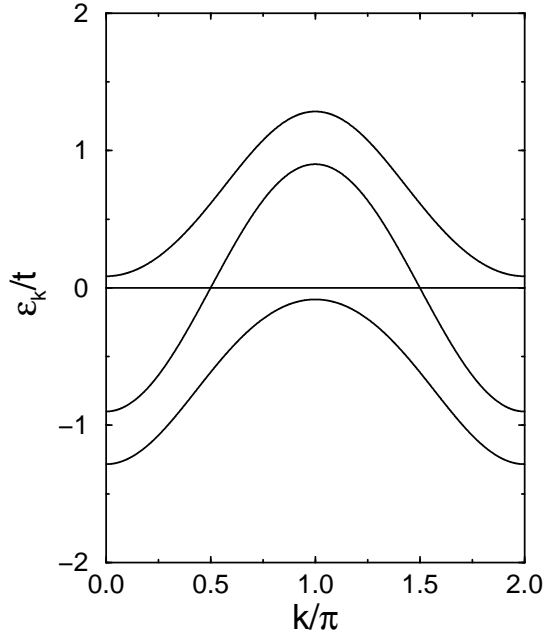


FIG. 13. Holon bands for a single hole obtained by the mean field theory. The outer bands are the even-parity bands (bonding and anti-bonding) and the center band has odd parity (non-bonding).

The single particle spectrum is incoherent, because the excitations are composed of the annihilation of a spinon and the creation of a holon. We define the single hole Green's function as a matrix

$$G_{\nu\nu'}(k, \omega) = - \int dt e^{-i\omega t} \langle T(c_{k,\nu,\sigma}^\dagger(t) c_{k,\nu',\sigma}(0)) \rangle \quad (13)$$

where the indices ν and ν' denote the three legs of the ladder (T the time-ordering operator).

Decomposing the c -operators into spinon and holon parts we obtain the convolution

$$G_{\nu\nu'}(k, \omega) = \frac{1}{L} \sum_q \int d\omega' G_{\nu\nu'}^f(k+q, \omega+\omega') G_{\nu\nu'}^b(q, \omega') \quad (14)$$

with

$$\begin{aligned} G_{\nu\nu'}^f(k, \omega) &= - \int dt e^{-i\omega t} \langle T(f_{k,\nu,\sigma}^\dagger(t) f_{k,\nu',\sigma}(0)) \rangle \\ G_{\nu\nu'}^b(k, \omega) &= - \int dt e^{-i\omega t} \langle T(b_{k,\nu}(t) b_{k,\nu'}^\dagger(0)) \rangle \end{aligned} \quad (15)$$

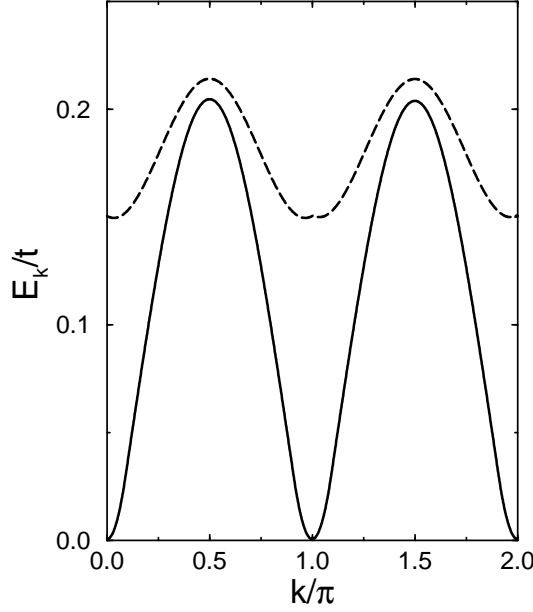


FIG. 14. Low-energy spectrum for a single hole obtained by the mean field theory.

The spectrum is obtained by diagonalizing the Green's function with respect to the leg indices. We show in Fig. 14 the lowest one-hole states for given momenta and parity analogous to the numerical results in Fig. 5. The spectrum changing the parity with respect to the groundstate of the half-filled system has gapless excitations at momentum $k = 0$ and π . This corresponds to the LL component of the three leg ladder. The states which keep the parity of the groundstate, however, are gapped with minima at $k = 0$ and π . In our mean field calculation the latter excitations lie above the LL spectrum, in contrast to the numerical result. The reason is that in the mean field treatment these excitations are almost exclusively carried by the spinon part, i.e. we remove a spinon in the lower even-parity spinon bands, while the holon remains in the lowest even-parity band. In the numerical calculation this spectrum lies clearly lower and cannot be identified directly with

spinon excitations which are higher in energy. Therefore, we conclude that our mean field calculation overestimates the splitting of the holon bands. Nevertheless, we can interpret both types of excitations consistently with the numerical calculations. In particular, we emphasize that the gapless spinons are in both treatments in odd-parity channel giving a consistent picture of the symmetries of the ground state and the low-lying excitations.

C. Finite doping

The analysis of our numerical data led us to the conclusion that there would be a finite range of doping close to half-filling where the LL state would coexist with the ISL. Beyond a critical doping δ_c the ISL would be doped and the whole system would turn into a LE where all channels open a spin gap. We might hope to describe this behavior within our mean field picture. However, in this treatment the mean field LL state is immediately unstable against the formation of a LE state, and there is no obvious transition between two different phases.

As soon as we introduce a finite concentration of holes in the system, the holons are described by a Bose-condensate in the mean field groundstate. Consequently, the single-particle Green's function consists of a coherent and an incoherent part due to the presence of the condensate,

$$G_{\nu\nu'}(k, \omega) = C_{\nu\nu'} G_{\nu\nu'}^f(k, \omega) + G_{\nu\nu'}^{\text{inc}}(k, \omega) \quad (16)$$

where $C_{\nu\nu'}$ is a constant proportional to the doping concentration δ . Thus, we find conventional Fermi liquid quasiparticles in the single particle spectrum. This has implications on the pairing in the doped ladder. The exchange term in the t - J model allows to scatter spin-singlet pairs of electrons between the even-parity and odd-parity channel. The relevant terms are derived from the exchange terms along the two outer legs, $J \sum_1 (\mathbf{S}_{i,1} \cdot \mathbf{S}_{i+1,1} + \mathbf{S}_{i,3} \cdot \mathbf{S}_{i+1,3})$, and become in electron operator formulation,

$$H_{+-} = \sum_{k,k',q} \sum_{\sigma=\uparrow,\downarrow} v_{k,k',q} [c_{k+q+, \sigma}^\dagger c_{k'+, -\sigma}^\dagger c_{k-, -\sigma} c_{k'+q-, \sigma} + c_{k+q-, \sigma}^\dagger c_{k'-, -\sigma}^\dagger c_{k+, -\sigma} c_{k'+q+, \sigma}]. \quad (17)$$

with $v_{k,k',q} = -J(\cos q + \frac{1}{2} \cos(k - k'))$. The even-parity channel corresponds to the ISL phase which is not populated by holes at small doping. However, via virtual scattering of hole pairs into the even-parity channel an effective pairing interaction for the holes in the odd-parity channel is generated, in lowest order given by

$$\begin{aligned}
V_{k,k'} &= -2i \sum_{k''} \int d\omega v_{k,k'',k+k''} G_{++}^f(k'', \omega) G_{++}^f(-k'', -\omega) v_{k',k'',k'+k''} \\
&= -\frac{J^2}{2} i \sum_{k''} \int d\omega (9 \cos k \cos k' \cos^2 k'' + \sin k \sin k' \sin^2 k'') G_{++}^f(k'', \omega) G_{++}^f(-k'', -\omega)
\end{aligned} \tag{18}$$

where $G_{++}^f(k, \omega)$ is the spinon Green's function in the even-parity channel corresponding to $G_{++}^f = \frac{1}{2}(G_{11}^f + G_{13}^f + G_{31}^f + G_{33}^f)$ from Eq.(15). In weak coupling theory this leads to the instability equation (ladder approximation) in the odd-parity channel,

$$1 = -k_B T \sum_{k,n} V_{k,k} G_{--}(k, \omega_n) G_{--}(-k, -\omega_n) \tag{19}$$

for finite temperature ($G_{--} = G_{11} - G_{13} - G_{31} + G_{33}$, and ω_n are the fermionic Matsubara frequencies). Since the Green's function has a standard quasiparticle pole as shown above in Eq.(16), we find a usual Cooper instability and a non-vanishing transition temperature for any finite coupling and density δ (note that G is proportional to δ). Thus, holes in the odd-parity channel would be paired in the groundstate. This is in contrast to the expectation for a LL where a critical coupling strength exists below which the LL remains stable [23]. Thus, this instability of the LL for any non-zero concentration of holes is a deficiency of the mean field description. On the other hand, it clearly indicates the trend towards pairing due to the coupling of the LL to the insulating or doped spin liquid which occupies a part of the spectrum. The RVB correlation of the ISL provides a pool of “preformed pairs” which triggers the instability of the LL towards the LE [24].

Although there is no obvious (non-zero) critical concentration where the character of the groundstate changes within the mean field treatment, we observe an interesting crossover between two regimes in the BCS mean field for the holes,

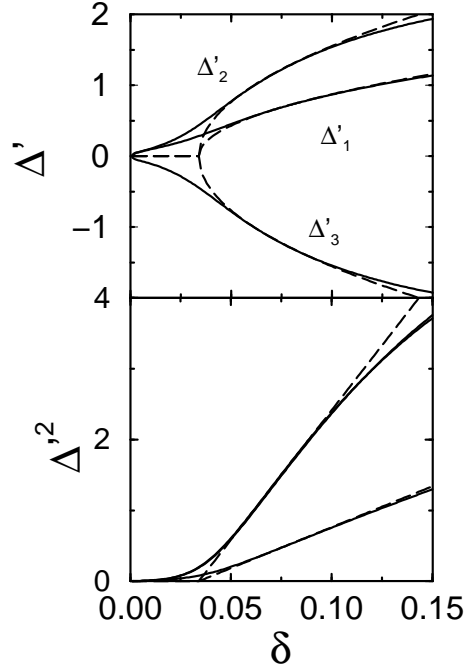


FIG. 15. The superconducting mean fields for finite doping. The solid lines correspond to the mean field calculation. The dashed lines are fits of the crossover assuming an underlying $\sqrt{\delta - \delta_c}$ -dependence of Δ' with $\delta_c \approx 0.034$. In the lower figure a linear fit is possible for Δ'^2 .

$$\Delta'_{ij} = \langle c_{i\uparrow} c_{j\downarrow} \rangle = \langle b_i^\dagger b_j^\dagger \rangle \langle f_{i\uparrow} f_{j\downarrow} \rangle = B_{ij} \Delta_{ij}. \quad (20)$$

The behavior of Δ' and Δ'^2 as a function of δ is shown in Fig. 15. The crossover indicates a critical concentration $\delta_c \approx 0.034$ (for $t = 2J$) found by extrapolation of the square root dependence of Δ' ($\propto \sqrt{\delta - \delta_c}$). For $0 < \delta \ll \delta_c$ Δ' is rather small as can be understood from Eq.(15) and (16). For small doping the dominant contribution to $V_{k,k'}$ originates from $k'' \approx \pm\pi/2$ the momenta for the spin gap in the even-parity channel and the Fermi points in for the odd-parity holes are close to $\pm\pi/2$ as well. Therefore the cosine-term in $V_{k,k'}$ contributes only little. This changes with increased doping where both the Fermi points and the lowest even-parity spinon energies are located at momenta gradually shifting away from $\pm\pi/2$. This leads to an effective enhancement of the pairing interaction as an effect of doping which yields the pronounced crossover whose symmetry aspects we discuss below. We expect that the same tendency is at work in the real system where in the very small

doping regime the effective interaction is sufficiently reduced to avoid pairing in the LL. Only with increased doping both the enhanced attractive interaction and the density of states at the Fermi level drive the system into the paired state.

Finally we would like to characterize this crossover by considering the symmetry of the gap function in momentum space. Thus, we introduce transverse momenta k_\perp along the rung. The bonding, antibonding and non-bonding states as given in Eq.(2) and (3) can be related to momenta k_\perp by using the following form for the dispersion,

$$\epsilon_{k,k_\perp} = -2t(\cos k + \cos k_\perp), \quad (21)$$

resulting from fixed boundary conditions along the rung. With Eq.(2) and (3) we find the correspondence: $b \rightarrow k_\perp = \pm\pi/4$, $nb \rightarrow k_\perp = \pm\pi/2$ and $ab \rightarrow \pm 3\pi/4$. Then we obtain for the momentum dependent gap function,

$$\begin{aligned} \Delta'_{k,k_\perp} &= \langle c_{k,k_\perp\downarrow} c_{-k,-k_\perp\uparrow} \rangle \\ &= -(2\Delta'_1 \sin^2(k_\perp) + \Delta'_2 \sin^2(2k_\perp)) \cos k - \Delta'_3 \sin(2k_\perp)(\sin(k_\perp) + \sin(3k_\perp)). \end{aligned} \quad (22)$$

We can use this form now to show the phase of the gap function in the first Brillouin zone (BZ). We observe that the gap function is basically positive along the k -direction ($|k_\perp| \ll \pi$) and negative along the transverse momentum direction k_\perp ($|k| \ll \pi$). This is essentially the structure of a “ $d_{x^2-y^2}$ -wave” pairing function. This is also reflected in real space where the gap function along the legs is positive (Δ'_1, Δ'_2) and along the rungs is negative (Δ'_3) as shown in Fig. 15. It is interesting to compare the position of the nodes in the two regimes separated by δ_c . For $0 < \delta \ll \delta_c$ we find that the gap functions have practically the same magnitude on all bonds. With this property Eq.(22) leads to nodes which correspond exactly to the [110]-direction in the BZ and we might consider this state as “purely” $d_{x^2-y^2}$ -wave like (see Fig. 16). On the other hand, for the regime $\delta > \delta_c$ the gap functions have the relation $\Delta'_1 < \Delta'_2 = -\Delta'_3$ which yields nodes clearly shifted away from the [110]-direction. We may consider this as an admixture of an (extended) s-wave-like component to the d-wave gap,

although, strictly speaking, the underlying symmetries are not present in the ladder system to justify the distinction between s- and d-wave pairing.

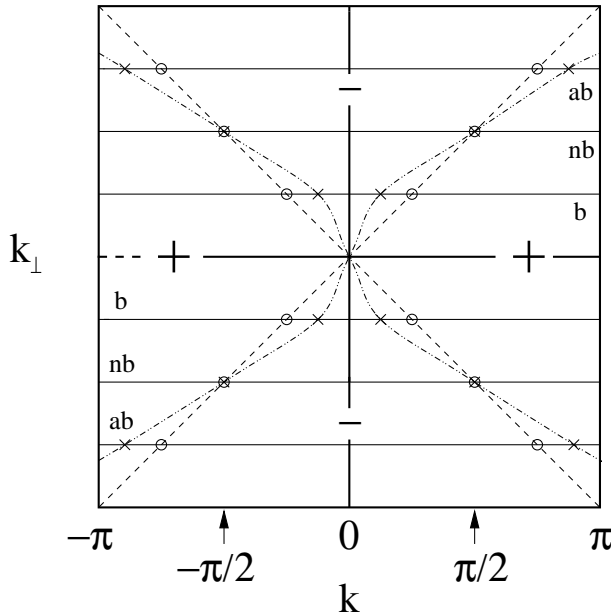


FIG. 16. Nodelines for the BCS gap, Eq. (22), in the first Brillouin zone. The dashed line connecting the empty circles shows the nodelines for $\delta = 0.01$. The dotted-dashed line connecting the x-marks gives the nodelines for $\delta = 0.06$. We define the transverse momenta k_{\perp} by $b \rightarrow \pm\pi/4$, $nb \rightarrow \pm\pi/2$, and $ab \rightarrow \pm3\pi/4$.

The difference of the two regimes may therefore be interpreted in the following way. The mean field superconducting state in the small doping regime is mainly carried by the even-parity channel and the odd-parity channel participates weak through proximity. Contrary to the exact numerical diagonalization, in the mean field treatment we cannot avoid the population of the ISL by holes strictly even at very small doping concentrations. The three-leg structure is apparently wide enough to create a LE state with a gap structure which is approximatively d-wave like. In the larger doping regime, however, the LL of the odd-parity channel acquires its own hole pairing so that an additional symmetry lowering occurs reflecting the 1D nature of the LL and generates an s-wave like additional component as seen in the shift of the nodelines (Fig. 16). Since there is no real symmetry distinguishing s- and d-wave from each other this transition appears only as a crossover when the interaction among

holes become strong enough in the (odd-parity) LL. This behavior is again in qualitative agreement with the interpretation obtained from our numerical calculation.

VI. CONCLUSIONS

The three-leg ladder is specially interesting because in a certain sense it combines two quite different elements - an odd-parity channel which behaves like a single chain, and two even-parity channels which behave similar to the two-leg ladder. This result is already foreshadowed in the undoped limit where the low-energy degrees of freedom can be mapped onto a single Heisenberg $S=1/2$ chain with longer range interactions, and the remaining transverse spin degrees of freedom have a substantial energy gap. In this work, we show that the initially doped holes enter only this odd-parity channel and form a Luttinger liquid, so that the system has two distinct components - the conducting Luttinger liquid in the odd-parity channel, and the insulating spin liquid in the even-parity channel. This phase we denoted as LL + ISL, and the numerical evidence from the Lanczos diagonalization of small clusters reported here and the DMRG calculations of White and Scalapino [10], that such a phase exists up to a critical hole density, δ_c , is we believe quite clear. In addition, we introduced a mean field approximation scheme which gave similar but not identical results. Initially, holes enter only the odd-parity channel which is gapless in the undoped system. However in the mean field approximation, a small gap develops in the odd-parity channel upon doping. This - as we discussed - reflects the inadequacy of the mean field description of the Luttinger liquid.

The LL + ISL phase has unusual properties. First of all, we note that the different parity channels of the original Fermi surface behave quite differently, so that only in the odd-parity channel is there a Fermi surface. The truncation of the Fermi surface in the partially occupied even-parity channels is not a consequence of a breaking of translational symmetry since the spin order here is purely short range. Rather it is a consequence of the proximity to the Mott insulating phase which in this channel is ISL. This truncation of some partially occupied

bands is a clear violation of Luttinger's theorem. Usually if one approaches a Mott insulator which has AF order, then one may proceed through incommensurately ordered phases which progressively truncate the Fermi surface, but do not violate Luttinger's theorem. However this option is not available if one approaches an RVB Mott insulator which is an ISL. However the example of the three-leg ladder shows us that here also a partial truncation of the Fermi surface is possible, but now it violates the Luttinger theorem.

This LL + ISL phase has certain features in common with a recent proposal by Geshkenbein, Ioffe, and Larkin (GIL) for the underdoped spin gap normal phase of the cuprates. They argue that the spin pairing implied by the spin gap did not cause immediately hole pairing. Instead they broke up the Fermi surface into two distinct parts - a fermionic part and a paired bosonic part. The latter they argued should have infinite mass to prevent conductivity from these bosons, and they associated this with the van-Hove singularity. In our specific example, the spin pairs are also insulating, but the origin lies in the proximity to the Mott insulating phase. In both models, the coexistence of fermionic and bosonic degrees of freedom leads to processes whereby a fermionic Cooper pair can scatter in and out of the bosonic channels, which however lie at higher energy. In a LL, there is no Cooper instability for an infinitesimal attraction, and a finite attraction is required for pairing. For this reason we believe a LL + ISL phase is possible in the three-leg ladder. By contrast, as we discussed above, the mean field description of the odd-parity channel has a true Cooper instability due to the holons being Bose condensed, and as a result hole pairing occurs at arbitrarily small hole densities. In the case of two dimensions, where the Fermi surface channels or patches near to the saddle points, $(\pm\pi, 0)$ and $(0, \pm\pi)$, first become paired and insulating, it is clearly crucial whether the remaining fermionic part of the Fermi surface has a Cooper instability (as assumed by GIL) or not. A Cooper pairing instability leads to hole pairing in the groundstate as in our mean field description.

The experimental examination of the Fermi surface evolution has been made by ARPES (Angle-Resolved-Photoemission-Spectroscopy). However, as we have seen, the inverse process would be more illuminating, but it is much more difficult to realize experimentally. In

the electron addition process, as we have shown, the Fermi surface truncation is very evident, although sidebands do allow an electron addition on the even-parity channel which is in the ISL state. Nonetheless the total weight at low energies will vanish as the hole doping vanishes, and will be concentrated mainly in the fermionic part of the Fermi surface.

In the three-leg ladder at dopings beyond δ_c , the ISL is converted into a doped Luther-Emery liquid, and a LL + LE phase occurs. This phase will show hole pairing and power law correlations in the CDW and singlet superconductivity channels. As the mean field approximation shows, the pairing is in an essentially d-wave channel. In the mean field theory, the quantum phase transition at δ_c appears as a crossover where the hole pairing increases rapidly as the hole density increases.

We wish to thank V.B. Geshkenbein, R. Hlubina, L.B. Ioffe, P.A. Lee, S.R. White, and D. Scalapino for useful discussions, and acknowledge the Swiss National Science Foundation for financial support. In particular, M.S. is grateful for the support by the Swiss National Science Foundation through a PROFIL-fellowship.

REFERENCES

- * New address: Yukawa Institute for Theoretical Physics. Kyoto University, Kyoto 606-01, Japan.
- [1] E. Dagotto and T.M. Rice, Science **271**, 618 (1996), and references therein..
- [2] H. Schulz, Phys. Rev. B **53**, R2959 (1996); H. Schulz, cond-mat/9605075.
- [3] D.V. Khveshchenko and T.M. Rice, Phys. Rev. B **50**, 252 (1994).
- [4] E. Arrigoni, Phys. Lett. A**215**, 91 (1996).
- [5] L. Balents and M.P. Fisher, Phys. Rev. B **53**, 12133 (1996).
- [6] T. Kimura, K. Kuroki, and H. Aoki, Phys. Rev. B **54**, R9608 (1996); T. Kimura, K. Kuroki, and H. Aoki, cond-mat/9610200.
- [7] H.H. Lin, L. Balents, and M.P. Fisher, cond-mat/9703055.
- [8] M. Troyer, H. Tsunetsugu, and T.M. Rice, Phys. Rev. B **53**, 251 (1996).
- [9] C.A. Hayward and D. Poilblanc, Phys. Rev. B **53**, 11721 (1996).
- [10] S.R. White and D. Scalapino, Phys. Rev. B **55**, 6504 (1997).
- [11] M. Ogata, M.U. Luchini, S. Sorella, and F.F. Assaad, Phys. Rev. Lett. **66**, 2388 (1991).
- [12] P.A. Bares and G. Blatter, Phys. Rev. Lett. **64**, 2567 (1990); P.A. Bares, G. Blatter, and M. Ogata, Phys. Rev. B **44**, 130 (1991).
- [13] D.S. Marshall *et al.*, Phys. Rev. Lett. **76**, 4841 (1996).
- [14] B. Frischmuth, S. Haas, G. Sierra, and T.M. Rice, Phys. Rev. B **55**, R3340 (1997).
- [15] M. Greven, R.J. Birgeneau, and U.-J. Wiese, Phys. Rev. Lett. **77**, 1865 (1997).
- [16] B. Frischmuth, B. Ammon, and M. Troyer, Phys. Rev. B **54**, R3714 (1996).

- [17] Boundary conditions with open shell configurations strongly favor paired groundstates and skew the balance between paired and unpaired states.
- [18] As a consequence of the Marshall theorem, Heisenberg chains and odd-leg ladders with $L = 2, 6, 10, \dots$ have a groundstate wavevector $k=\pi$, while systems with $L = 4, 8, 12, \dots$ have $k=0$.
- [19] Note that this 2-hole LL + ISL state for PBC lies slightly higher in energy than the 2-hole LE state which has total momentum $k=0$, and a filled shell configuration in the nb -channel, i.e. 6 electrons with $k=0$ and $k=\pm\pi/3$ states fully occupied. We ascribe the extra stability of the LE state to this favorable filled shell structure.
- [20] M. Sigrist, T.M. Rice and F.C. Zhang, Phys. Rev. B **49**, 12058 (1994).
- [21] G. Kotliar and J. Liu, Phys. Rev. B **38**, 5142 (1988).
- [22] I. Affleck, Z. Zou, T. Hsu and P.W. Anderson, Phys. Rev. B **38**, 745 (1988).
- [23] A.V. Balatsky, Philosophical Magazine Lett. **68**, 251 (1993); Y. Ren and F.C. Zhang, Phys. Rev. B **52**, 536 (1995).
- [24] V.B. Geshkenbein, L.B. Ioffe and A.I. Larkin, Phys. Rev. B **55**, 3173 (1997).